Existence of a Traveling Wave Solution to Glioblastoma Multiforme Model with Modified Gompertz Growth Function

by

Gulnissa Zhuman

Submitted to the Department of Mathematics
in partial fulfillment of the requirements for the degree of

Master of Applied Mathematics

at the

NAZARBAYEV UNIVERSITY

Apr 2022

Author .....
Department of Mathematics
Apr 22, 2022

Certified by .....
Ardak Kashkynbayev
Assistant Professor
Thesis Supervisor

Accepted by .....
Gonzalo Hortelano
Dean, School of Science and Humanities

Existence of a Traveling Wave Solution to Glioblastoma Multiforme Model with Modified Gompertz Growth Function

by

Gulnissa Zhuman

Submitted to the Department of Mathematics
on Apr 22, 2022, in partial fulfillment of the
requirements for the degree of
Master of Applied Mathematics

Abstract

This thesis explores a model for aggressive brain cancer - glioblastoma multiforme, with modified gompertzian growth function. Density-dependent diffusion term, taxis, and growth functions are included in the model that considers the glioblastoma multiforme properties. The experimental data of Stein et al. [58] has been used in this work. The given model is solved both analytically and numerically by using the Matlab program. The analytical method finds the condition for existing a traveling wave solution of the given glioblastoma model and numerical computations are done by using the Nelder-Mead simplex algorithm that minimizes the function through which it finds the optimal parameters of the model. The simulation results confirm the analytical predictions.

Thesis Supervisor: Ardak Kashkynbayev
Title: Assistant Professor

Acknowledgments

First of all, I would like to express my sincere appreciation to my thesis supervisor Professor Ardak Kashkynbayev for his guidance, kind responsiveness, patience and constant encouragements throughout the course of this research project.

I would like to give special thanks to my Second Reader Professor Shirali Kadyrov from Suleyman Demirel University for helping me better understanding numerical simulation part as well as for his feedback and suggestions needed for improvements of my thesis.

This research is funded by the Science Committee of the Ministry of Education and Science of the Republic of Kazakhstan Grant AP08052345 ("Mathematical models for Glioblastoma proliferation"). I would like to acknowledge Professor Yang Kuang from Arizona State University, Professor Bibinur Shupeyeva from Nazarbayev University, and my colleagues from the research group - Aisha Tursynkozha and Daiana Koptleuova, for the fruitful discussions that we had during my master's degree, and for their valuable comments and advice.

Finally, I would like to thank my family, especially my sister Khalbinur Zhuman for her moral support and motivation during this process.

Contents

List of Figures

List of Tables

Chapter 1

Introduction

This thesis concentrates on analyzing density-dependent reaction-diffusion equation with Gompertzian growth function for one dimensional model

$$\frac{\partial u(x,t)}{\partial t} = \underbrace{\nabla \cdot \left(D\left(\frac{u}{u_m}\right) \nabla u \right)}_{\text{density-dependent diffusion}} - \underbrace{sign(x) v_i \nabla \cdot u}_{\text{taxis}} + \underbrace{\rho u \ln\left(\frac{u_m}{u+\alpha}\right)}_{\text{growth function}}. \tag{1.1}$$

In the model the Gompertz growth function

$$\frac{du}{dt} = \rho u \ln\left(\frac{u_m}{u}\right)$$

is modified by adding some value $\alpha > 0$ to ensure the maximum growth rate, otherwise the conventional Gompertz growth function states that the maximum growth rate is infinity which does not have a biological meaning. The Gompertz growth function has the following parameters: ρ - the intrinsic rate, $u(x,t)$ - the tumor invasive cells at a position x and time t, u_m is a carrying capacity and $\alpha > 0$ is a some positive value.

The main aim of this research is to study how fast the tumor grows and how it spreads in a certain amount of time both computationally and numerically. So, we

need to define the condition at which the traveling wave solution exists for density-dependent reaction-diffusion equation with a modified Gompertz growth function. To meet the goal, a traveling wave solution of the model (1.1) should be analyzed, which has density-dependent diffusion term, taxis and growth function. Density-dependent diffusion term states that the number of diffusion depends on the number of cells, taxis describes the migration of the tumor cells from the tumor core and modified Gompertz growth function demonstrates the tumor growth. Here u is the tumor invasive cells at a position x and time t, u_M is the carrying capacity, ρ is the intrinsic rate and v_i is the cells migration degree at which they migrate away from the core.

Traveling wave solution is given by the form

$$u(x,t) = h(x - ct) := h(y),$$

where $y = x - ct$ is the *wave variable*, x is a spatial domain, t is a time domain and c is a speed of a wave.

Diffusion function that is used in this work is

$$D_1 - \frac{D_2 u^n}{a^n + u^n},$$

where D_1, D_2, a, n are parameters that satisfies these conditions $D_1 \geq D_2, n \geq 1, a > 0$, and u is the cell density. The parameter n shows how considerably the diffusion function reduces while the parameter a identifies the cell density u which ensures the movement at half maximum rate. Diffusion function satisfies the following conditions:

- $D(u)$ is a continuous and differentiable function;
- $D(u)$ is a positive and decreasing function for $u \geq 0$.

The important result of this paper is proving the existence of a traveling wave

solution for density-dependent reaction-diffusion equation with a modified Gompertz function when the minimum wave speed is satisfied.

Theorem. *There exists a traveling wave solution in the form*

$$u(x,t) = h(x - ct) := h(y)$$

of density-dependent reaction diffusion equation

$$\frac{\partial u}{\partial t} = D(u)\frac{\partial^2 u}{\partial x^2} + D'(u)\left(\frac{\partial u}{\partial x}\right)^2 - p\frac{\partial u}{\partial x} - u\ln(u+\alpha).$$

that satisfies the boundary conditions $u(x,t) \to 1$ *as* $x \to -\infty$ *and* $u(x,t) \to 0$ *as* $x \to \infty$ *with* $0 < u(x,t) < 1$*, whose orbit connects the steady states* $u = 0$ *and* $u = 1 - \alpha$ *if and only if*

$$c \geq c_{min} = \frac{v_i}{\rho} + 2\sqrt{-\ln(\alpha)D(0)}.$$

is satisfied.

Moreover, sensitivity analysis of parameters is conducted and numerical results with obtained optimal parameters are compared with the experimental data of [58]. In addition, the total errors of [59, 31] and this work are compared with each other.

Therefore, the outline of the thesis is as follows. We begin the next chapter by providing a general background to glioblastoma multiforme cancer type, giving a definition of traveling wave solution, discussing reaction-diffusion equations as well as growth functions. Also, we explain each step of Nelder-Mead algorithm which is applied in simulation part. In chapter 3, we re-write the model in one-dimensional Cartesian coordinates and then by applying some mathematical operations we obtain a system of first-order ordinary differential equations. Next, we calculate its fixed

points and compute Jacobian matrices at that steady-states to find the stability of each steady state. Following that the heteroclinic connection between these points will be found. Chapter 4 provides numerical results of the model obtained via Matlab program. The optimal parameters of the model are found and numerical solution of the Gompertzian model is compared with the previous studies [59, 58]. In chapter 5, the findings of analytical and numerical analysis are discussed. Chapter 6 makes conclusions based on the results and draws the general ideas on which the future research might be based on.

Chapter 2

Preliminaries

2.1 Mathematical Modelings in Biology

The mathematical models are a crucial tool that can be constructed for simulating predator-prey, competition interactions, renewable resource management pest control strategies, multispecies societies, growth of the tumor, growth of the bacteria, and for many other biological processes [45]. As Shonkwiler and Herod [55] state, mathematical models study the questions regarding biological processes which can be tested only in real biological systems. So, mathematical models help to understand the mechanisms of biological processes and ensure to do their practical predictions.

A classical way of modeling cancer diseases is by using systems of ordinary differential equations and partial differential equations. Systems of ordinary differential equations well describe qualitative and quantitative characteristics of cancer within the body. One of the earliest mathematical model of tumor growth was introduced by Greenspan in 1972 [23]. The tumor growth in the development's avascular stage was simulated via a nutrient diffusion and an internal pressure. Greenspan's model predicts that after some time the tumor will have different parts as necrotic, quiescent, and proliferative. Necrotic forms at the center of the tumor, quiescent form appear as

a ring around the necrotic core, and proliferative form, which appears as a thin layer of cells, arises around the quiescent area. The tumor growth in the development's avascular stage was simulated via a nutrient diffusion and an internal pressure. From the results, the author concluded that the decreasing of necrotic cells allows cells to move inward due to the internal pressure. To investigate the behavior of a radially symmetric benign tumor which can modify to become a malignant and invasive tumor at the avascular stage because of the loss of cell-cell adhesion, the work of Greenspan was re-studied and extended by Byrne and Chaplain in 1996 [6]. Their reaction-diffusion model considers an avascular solid tumor that has only proliferating cells and whose growth rate determined by an externally supplied nutrient such as oxygen and glucose. In 2011 Stiehl and Marciniak-Czochra formulated a model of ODE's system that describes the lineage structure of the hematopoietic system in the body [60]. The model assisted to divide the blood population into three separations which are stem cells, mature cells and progenitor cells. The outcome of the experiment depicted that it was possible to find a steady state that could describe the quantity of each blood cell existing in the human body. The mathematical model was later modified by involving a stem cells based cancer model with normal blood cells in order to study the development of leukemia. The ODE model exactly depicts the system dynamics even though the blood cells are well mixed within the body. However, ODE models cannot describe events that happen in various spatial locations or locations where cells are migrating. For example, glioblastoma multiforme both proliferate and migrate which makes for a system of ODEs very challenging to capture the features of glioma cells. To capture these features one should use a partial differential equations model which includes additional independent variables like taxis, diffusion term and growth function.

Application of mathematics in biology and medicine was proposed by a few people

in the distant past and only in the last centuries it was actively applied and analyzed by scientists [44]. One of scientists who studied mathematical biology was Bernoulli who did a great contribution to early application of mathematical models in medicine by introducing a differential equation model which examined the efficiency of vaccination against smallpox [3]. According to J. Murray [44], if the work of Bernoulli had been published at the beginning of the 20th century, it would have been considered one of the great improvements in mathematical biology along with the papers of Lotka [40] and Volterra [70] on modelling predator–prey interaction in the population of organisms, Fisher [21] on the genetics of natural selection, Kermack and McKendrick's [32] article on modelling epidemics, and Fisher [20] and Kolmogoroff et al. [34] who brought diffusion into their mathematical models of certain biological phenomena.

The first and only biologically-derived growth model was introduced by von Bertalanffy in 1938 [71] whose purpose was to model the growth of guppies in terms of length and mass. His equation gives a chance to slow the rapid initial growth without inflicting rigorous asymptotical conditions. Despite the fact that at the beginning of 1950s von Bertalanffy suggested to use the equations in modeling cancers, it was infrequently used in that field.

In the late 1960s and at the beginning of 1970s the interest in mathematical biology dramatically increased, in particular reaction-diffusion systems were heavily studied theoretically. The work of Prigogine and Nicolis [51] is a great example of it. Their work considered an instability in purely dissipative systems involving chemical reactions and transport processes such as diffusion.

Another application of mathematics in biology is the Xue et al.'s model [73] which originally meant to determine therapeutic strategies that could help cure ischemic wounds. The model itself is in the form of partial differential equations system which includes the main variables involved in the healing process, specifically, several types

of blood and tissue cells, chemical signals as well as density of the tissue. Thanks to the model of Xue et al. needs on making and testing hypotheses on animals were noticeably reduced, which shows the model's significance on healing process by being a tool to suggest biologically testable assumptions.

2.2 Human Oncology

Cancer is a disease from the past that still afflicts people today. As stated in [24, 61], "cancer" is a Greek word that was used by Hippocrates to describe carcinoma tumors, however, he was not the first to discover cancer diseases. The world's oldest printed cancer case report was published as a 54-page booklet in 1507 [25]. The report contained 19 non-cancerous cases compiled by a practicing physician and surgeon Antonio Benivieni. Benivieni tried to cure the patient, who was his relative, from vomiting and wasting, but the treatment was not giving any result. By abdominal incision of the patient he found thickened and nodular gastric folds as well as firm stomach induration which caused complete obstruction of the pylorus. Despite of the fact that Benivieni did not define it as carcinoma and did not investigate the abdomen, all these descriptions coincide with the gastric carcinoma. Thus, such contributions that were made during the period of 1500-1750 in pathology and surgery are considered the foundation for future understanding of the nature of malignant and benign tumors in the 18th and 19th centuries [26].

In 1972 Greenspan [23] modeled the growth of solid carcinoma with nutrient diffusion. He stated that the tumor was in the shape of a sphere and it had three layers: a central necrotic core, viable non-proliferating cells, and the outer layer where all mitosis takes place. Another model was created by Murray and Frenzen in 1986 [22] to give a justification for Gompertz's growth function based on a model introduced by Rubinow [53] about cell kinetics. Their model depicts the population of a cell where

every cell is described by a degree of maturation. Correlation between cell doubling time and cells' growth pattern is examined in the Frensen-Murray model.

Another eye-opening paper was written by Burgess et al. [5] where they presented a three-dimensional model that is used nowadays as the basis for three-dimensional models. Burgess et al. were the first to state in their work that the major component of glioma growth is a cancer cell diffusion. Additionally, they demonstrated that only tumors with a low diffusion rate may be cured from a surgical resection. Thanks to the contributions of Collins et al. [9] and of Steel [57] there has been numerous developments in mathematical modeling in the field of human oncology. The growth rates of a radiographically measurable metastatic lung disease in adults as well as a kidney cancer that mostly affects children - Wilms's tumor, were investigated in the Collins et al. paper. The obtained results show the existence of exponential tumor growth as well as the applicability of relevant concepts in justifying many vague parts of human neoplastic diseases. In the next decennial in addition to the contribution of Collins et al., Steel defined the concept of a cell kinetic parameter and included in the vocabulary of radiation biologists and oncologists. As stated by Steel, the time change between tumor doubling volumes shows a significant volatility among tumors with various histology and between primary and metastatic lesions.

In 2001 de Pillis and Radunskaya [13] constructed competition model by using ordinary differential equations of an immune system and a drug therapy. Their model describes the interaction between those cells: immune cells, tumor cells and host cells. The authors concluded that the coexisting equilibrium is very sensitive to the tumor response rate and the source rate of the immune cells. The authors concluded that the coexistence equilibrium depends on the tumor response rate and the source rate of the immune cells.

According to Global Cancer Observatory - *Cancer Today*, cancer is the most fatal

Grade	*WHO designation*	*Characteristics*
WHO grade I	Pilocytic astrocytoma	• Least malignant • Possible curable • Non-infiltrative • Long term survival • Slow growing
WHO grade II	Astrocytoma (Low grade)	• Relatively slow growing • Somewhat infiltrative • May recur as higher grade
WHO grade III	Anaplastic astrocytoma	• Malignant • Infiltrative • Tend to recur as higher grade
WHO grade IV	Glioblastoma multiforme	• Most malignant • Rapid growth, aggressive • Widely infiltrative • Rapid recurrence

Table 2.1: Brain Tumor Grades according to World Health Organization [33].

disease that accounts about 9.96 million death cases, which is almost 52% of all incidents in 2020 worldwide [19]. The World Health Organization (WHO) grades brain tumors to estimate a tumor's malignancy by levels I-IV (see Table 2.1). Tumors are classified based on grades as a low-grade *(corresponds to the tumors of WHO grade I and II)* and a high-grade *(corresponds to the tumors of WHO grade III and IV)*. Low-grade brain tumors are non-cancerous, slowly growing and they usually do not spread, while the high-grade brain tumors are cancerous, fast growing and they can also grow into nearby tissues as well as spread within central nervous system.

Therefore, as it is easily understood, the tumor corresponding to grade I is the least malignant tumor, while the most malignant and invasive tumor fits to grade IV.

Despite of the fact that there are over 100 types of cancer, malignant brain cancer is the leading catastrophic cancer type which is the most frequent cause of children's and adult's mortality [41]. Tumor cells of malignant brain cancer have vague borders and rapid progression rates since they easily attack neighboring cells in the brain or even in the spinal cord [63]. Since the early detection of brain cancers is almost impossible and difficult, the chance of cure for patients with this type of cancer is extremely poor [31]. Nevertheless, it is hardly known that 81% of brain tumours is formed by gliomas [50] and 47% of all glioma diseases are the cases of fourth grade of gliomas - glioblastoma multiforme [2].

2.3 Glioblastoma Multiforme (GBM)

Glioblastoma multiforme (GBM) is one of the most common and aggressive brain cancers which grows and formulates its form in three months [11]. Humans with GBM cancer type die faster in comparison with other cancer diseases and mostly do not have a chance to have a long treatment, since most of them live only approximately 14 months since a cancer has been detected in their body [29, 1]. Due to the characteristics of glioma cells, GBM is hard to treat, since they proliferate and migrate intensively. Unfortunately, the tumor core can be removed only by surgical resection which does not remove migratory cells, as a result this leads to ineffective treatment. Nonetheless, different characteristics of gliomas allow to predict their growth stage and invasive properties, and models assist to visualize how these attributes behave. According to Dieckman [17], growth of GBM has been discovered since 1937 and can be described by the reaction-diffusion equations as well as proliferative-invasive models. Most of GBM models that were considered earlier are in the form of reaction-

diffusion equations and this is because of the fact that such equations describe exactly tumour spatiotemporal dynamics. The first reaction-diffusion models of GBM capture the proliferating tumor core. This was studied by Tracqui et al. [65] and improved by Swanson et al.[62]. The former introduced a model which describes glioblastoma growth and diffusion with therapeutic intervention, while the latter upgraded the equation by taking into account a spatially dependent diffusion in order to better the behaviour model of migratory tumor cells.

2.3.1 Biological background of glioblastoma

Glioblastoma multiforme in 90% of GBM cases emerges as a *de novo*, i.e. primary GBM which develops tumors from glial cells in the brain. The rest 10% of the cases develops from a lower-grade astrocytomas through time which progress to a high-grade that can obtain glioblastoma characteristics. The most appeared location of the tumor is the frontal and temporal lobes as well as the other supratentorial parts of the brain, but it can also be located in the brainstem, cerebellum and spinal cord [15].

As stated by Liu et al., the origin of GBM cells are still a subject of an ongoing research. There is a suggestion that cells found in the brain are cancer cell-of-origin; in fact, those cells are called neural stem cells (NSCs) since they have features of stem cells [39]. Stem cells are recognized as a self-renewal that can differentiate into other cell types. Creating and supporting the functioning organ is the main purpose of them [54]. They are defined as a cancer cell-of-origin due to the fact that tumors' locations connect to the subventricular zone, where adult NSCs stay. The cancer stem cells display fundamental behavior of being capable to form tumors when implanted to the mice with weakened immune system. This results in tumors that show resemblance with the phenotype and reiterate all cell types found in parent tumors. Thus, the

cancer stem cells may be a motive power in the growth of glioblastoma multiforme due to their limitless growth potential [12].

As it is said earlier, GBM can both migrate and proliferate, but those migratory and proliferating cells differ from one another. In order to migrate, cell shapes must be changed to cooperate with the extracelluar matrix and to become polarized as well as to develop extensions of the membrane [18].

2.3.2 Mathematical background of glioblastoma

The foundation for a mathematical model began to take form starting from the initial research on dynamics of glioma growth. The formulation of the model was transformed and modified every time as a series of models were developed and every next model was improved in comparison to the previous one. A modified form of the first glioblastoma multiforme model is well-known Fishers equation [62, 46]. This equation was introduced by R. A. Fisher in 1937 in his paper "The wave of advance of advantageous genes" and it is known as an ecological model of logistically growing population with simple Fickian diffusion. The equation is shown below:

$$\frac{\partial u}{\partial t} = g(u) + D\frac{\partial^2 u}{\partial x^2}, \tag{2.1}$$

where $g(u) = \rho u\left(1 - \frac{u}{u_m}\right)$ is the logistics growth function. Here u is the cell density, ρ is the intrinsic rate, u_m-carrying capacity and D is the cell diffusion rate. Since author tried to model the spread of an organism, he looked at the traveling wave solution of the form

$$u(x,t) = u(x - ct) = u(z). \tag{2.2}$$

After a laborious work he concluded that if the wave speed is $c \geq 2$ [35], then there exists a traveling wave solution of the form (2.2). After analyzing the model the

researcher found that the model has two equilibrium points: (0, 0) and (1, 0). Then by using Canosa's approximation method [8] the heteroclinic connection in the phase plane as well as physical plane were considered. The obtained results are least accurate when $c = 2$ and only first terms of series give a few per cent accuracy even if the minimum wave speed was satisfied.

The basic mathematical model defined by Murray's group [46] based on the classical definition of cancer consists of two key components of the tumor growth in the following equation written in words:

$$\begin{aligned}\text{rate of change of glioma cell density} &= \text{diffusion (invasion) of glioma cells} \\ &\quad + \text{net proliferation of glioma cells},\end{aligned} \tag{2.3}$$

which can be mathematically represented as follows

$$\frac{\partial u}{\partial t} = \nabla \cdot (D \nabla u) + \rho u. \tag{2.4}$$

One can notice that the Fisher's equation exactly coincides with the basic model given by J.Murray's group. The equation above describes the dynamics of tumor cells where $u(x, t)$ is the tumor cell density at position x and time t, D is a diffusion which describes net motility of tumor cells, ρ is a net proliferation of tumor cells, the symbol ∇ is the spatial differentiation operator. The conservation diffusion equation was created based on the fact that the gliomas almost never metastasize outside of the brain.

Stein et al. [58] analyzed glioblastoma tumor spheroids invasion model by focusing on the invasive cells in three dimensional case and created a continuum model which fits well the experimental data. Their mathematical model depicts seperate glioblastoma cells as the proliferating cells and the migratory cells and the model was created

based on in vitro experimental data that involves tumor spheroids formed by proliferation of two human astrocytoma cell lines. As for the Stein et.al's experimental data, the authors examined 16 different experiments and from that derived average invasive radii. U87WT and U87ΔEGFR glioma cell lines form multicellular spheroids embedded into self-assembled collagen-I gels augmented by minimum conditions of required environment and 2% fetal bovine serum. These spheroidal cells cultivated under standard cell culture conditions for 7 days and digital photomicrographs of the tumor spheroids were taken daily. Based on the experiment, a model introduced by Stein et al. describes the movement of invasive cells and they suggest that after leaving the tumor core, the tumor cells become invasive cells in order to enter the collagen gel. Therefore, the work of Stein et al. derived from the experimental data well depicts invasive cells' behavior in a way that one can compare its quantitave characteristics with the experimental measurements. Evolution of the invasive cell population can be described by four parameters as diffusion, taxis, shed cells as well as logistics growth function. This model is represented by the following equation:

$$\frac{\partial u_i}{\partial t} = D\nabla^2 u_i - v_i \nabla_r \cdot u_i + s\delta(r - R(t)) + g(u_i)\left(1 - \frac{u_i}{u_m}\right), \tag{2.5}$$

where D is the diffusion term, s is the core surface, g - proliferation, δ is the Dirac delta function, and r is the coordinate from the tumor center to the radial distance. The core radius is depicted as a linear function $R(t) = R_0 + v_c t$, in which R_0 - initial core radius, $v_c t$ - constant velocity at which core radius increases at time t. This model represents invasive cells $u_i(r, t)$ which diffuse and proliferate as others, but move away with the speed v_i from the tumor spheroid. Due to the diffusion term as well as Dirac delta function this model is complex and arduous for analyzing traveling wave solutions. By reason of this complexity Stepien et al. lightweighted the model by modifying it as follows:

$$\frac{\partial u}{\partial t} = \underbrace{\nabla \cdot \Big(D\Big(\frac{u}{u_M}\Big)\nabla u \Big)}_{\text{density-dependent diffusion}} - \underbrace{sgn(x) v_i \nabla \cdot u}_{\text{taxis}} + \underbrace{g(u)}_{\text{growth function}} . \tag{2.6}$$

Since authors considered tumor core with an invasive cells, there is no need of cell shedding term and therefore it was removed from modified model's version (2.6). The diffusion is changed for density-dependent diffusion term since there are some models which contain such diffusivity (for an example read [7]). Since the tumor cells increase, the existence of logistic growth function is meaningful in this equation as well as taxis term, which describes the migration of tumor cells from tumor core.

In the works of Stepien et al. and Kashkynbayev et al. [59, 31], they used reshaped GBM model of density-dependent reaction diffusion equation with logistics and Bernoulli's growth functions respectively. Stepien et al. used logistic growth function since it is mathematically sensible due to the simplicity of the form, whereas Kashkynbayev et al. believed that Bernoulli growth function fits the data equally as logistics do since it is a general form of logistic growth function. They both considered a density-dependent convective-reaction-diffusion equation and analyzed traveling wave solution. In both cases Jacobian matrices of the system have two steady-state solutions: stable and saddle equilibrium points. Stepien et al. established that traveling wave solution of (2.6) with logistically growing population exists when $c \geq c_{min} = 2\sqrt{D_1 \rho} + v_i$. But Kashkynbayev et al. showed the existence of traveling wave solution under the condition of $c \geq c_{min} = 2\sqrt{D(0)\rho} + v_i$ for Bernoulli's model. In order to prove the existence of solutions, both authors needed to demonstrate a heteroclinic orbit connecting these two steady-state solutions. They summarized the results by providing and proving the theorem which states that the traveling wave solution exists if c_{min} is satisfied. Numerical simulations were provided too. They compared numerical results of the models with the experimental data from [58].

2.4 Traveling wave solution

According to Murray [45], *the traveling wave* is a wave that moves without change of shape. Thus, if we have a traveling wave solution $u(x,t)$, then the shape of the traveling wave solution will be the same for all time and the speed of the solution, c, will be constant. In [69], traveling wave solution is given by the form $u(z) = u(x,t) = u(x-ct)$, where $z = x - ct$ is the *wave variable*, x is a spatial domain, t is a time domain and c is a speed of a wave. So, if $x-ct$ is constant, so is $u(x,t)$. The traveling wave solution of the form $u(x,t) = u(x-ct)$ moves in a positive x-direction, while $u(x,t) = u(x+ct)$ moves in the negative x-direction. The traveling wave of a case when $c = 0$ is called *a stationary wave*. Such waves do not spread and generally noticed during inducing a fixed boundary. The traveling waves can be categorized by the properties that they have. A traveling wave that approaches constant which is given by $u(-\infty) = u_l$ and $u(\infty) = u_k$ where $u_l \neq u_k$ is called *a wave front*. But if the constant values are equal, $u_l = u_k$, then a traveling wave is called *a pulse wave*.

By traveling waves impulses in nerve fibres as well as shock profiles that in fluid dynamics of conservation laws are represented [46, 56]. The traveling wave solution is obtained by solving a model which mostly given in the form of partial differential equations in which the solution dynamics could be understood via finding the solution of a model.

A traditional way of finding traveling wave solutions of second order partial differential equations is re-writing the equations into second order ordinary partial differential equations by substituting traveling wave ansatz. Then, the equations are split into an autonomous system of two ordinary differential equations. Following that, equilibrium points, which are steady-states of the system, should be found and those fixed points should be analyzed for stability by linearizing the system of equations and finding the eigenvalues of Jacobian matrices corresponding to each steady states.

Theory of traveling wave solution became popular after contributions of Kolmogorov, Petrovskii, Piskunov and a basis for their work was done by the Zeldovich and Frank-Kamenetskii combustion theory which is well-known among chemical physicists. Another famous example of considering traveling wave solution is the Fisher equation, to the field where he made tremendous contribution [20, 34, 69].

So, let us consider Fisher equation (2.1)- the simplest case of performing phase plane analysis and showing the existence of traveling wave solution. By substituting ansatz of a traveling wave, one can re-write (2.1) in the following form

$$u'' + cu' + (u - u^2) = 0. \tag{2.7}$$

Then by taking $u' = v$, the next system of ordinary differential equations can be obtained

$$\begin{aligned} u' &= v, \\ v' &= -cv - (u - u^2). \end{aligned} \tag{2.8}$$

In order to find equilibrium points, one must equalize the right hand side of the system to 0.

$$\begin{aligned} v &= 0, \\ -cv &- (u - u^2) = 0. \end{aligned} \tag{2.9}$$

Then the fixed points are found which are $(u, v) = (0, 0)$ and $(u, v) = (1, 0)$. Next, we want to compute Jacobian matrix of the system

$$J = \begin{pmatrix} 0 & 1 \\ -1 + 2u & -c \end{pmatrix} \tag{2.10}$$

and in order to define the stability of the fixed points, we calculate the Jacobian matrix at each point and find eigenvalues of corresponding matrix

$$J(0,0) = \begin{pmatrix} 0 & 1 \\ -1 & -c \end{pmatrix}, \qquad J(1,0) = \begin{pmatrix} 0 & 1 \\ 1 & -c \end{pmatrix}. \tag{2.11}$$

The characteristic equation and the eigenvalues of $J(1,0)$ are given below

$$\begin{aligned} \lambda^2 + \lambda c - 1 = 0 \\ \lambda = \frac{-c \pm \sqrt{c^2+4}}{2}, \end{aligned} \tag{2.12}$$

which means that the equilibrium point $(1,0)$ is a saddle point for positive c (can be showed by Descartes's rule of signs). For the second equilibrium point the characteristic equation and the eigenvalues are

$$\begin{aligned} \lambda^2 + \lambda c + 1 = 0 \\ \lambda = \frac{-c \pm \sqrt{c^2-4}}{2}, \end{aligned} \tag{2.13}$$

where equilibrium point depends on the value of c. When $0 < c < 2$ the fixed point (0, 0) is a stable focus. When $c \geq 2$ the fixed point is a stable node which is more realistic traveling wave solution. So, the necessary and sufficient condition for existence of a traveling wave solution is $c \geq 2$, and this is the only case where the heteroclinic connection that connects two steady-state points, (0, 0) and (1, 0), exists.

2.5 Reaction-diffusion equations

The next significant terms of models are reaction and diffusion functions. Reaction-diffusion equations well describe the behaviour of different chemical and physical acts that happen around the world. Diffusion function is originally introduced for the

processes where the movement of molecules, atoms, heat from the high-concentration to a low-concentration part in order to maintain balanced concentration. In the term *"reaction-diffusion equations"*, the word *"reaction"* indicates the process where the concentration of the selected substance changes, in particular, how much substances are produced per unit volume per unit time, at the time when *"diffusion"* represents the procedure that describes the substance movement in space [10].

In 19th century, Adolf Fick mathematically described the diffusion process, which is now known as a Fick's law. The mathematical expression of diffusion is given by the following equation:

$$F = -D\nabla u, \tag{2.14}$$

where D is the diffusion coefficient, u is the concentration, and F refers to the rate of transfer per unit area [30, 52]. The negative sign means that there is a diffusion in the opposite direction to the concentration, while the positive sign describes the diffusion in the same direction as a concentration [10]. By using Fick's law, the usual form of the diffusion equation is

$$\frac{\partial u}{\partial t} = \nabla(D\nabla u). \tag{2.15}$$

If the diffusion coefficient D is a constant, then (2.15) can be written as the following

$$\frac{\partial u}{\partial t} = D\nabla^2 u. \tag{2.16}$$

Such equations describe the cases when the substance is created or destroyed inside of the region. However, there are situations where the stuff is being created or destroyed outside of the region and in order to deal with this problem reaction function is needed. In such cases the reaction function is added to the previous equation (2.16)

and obtains the next mathematical form:

$$\frac{\partial u}{\partial t} = D\nabla^2 u + r(u) \tag{2.17}$$

where $r(u)$ is the reaction function. This is the simplest case of reaction-diffusion equation which is also known as the Kolmogorov–Petrovsky–Piskunov (KPP) reaction-diffusion equation [4, 64]. The reaction function may vary and depends on the physical and biological phenomena. For instance, in Fisher equation (2.1) the reaction function is a well known logistics growth function. Another case is when reaction function is equal to $u(1-u^2)$ then the obtained equation will take a form of the Rayleigh–Benard convection equation

$$\frac{\partial u}{\partial t} = D\nabla^2 u + u(1-u^2). \tag{2.18}$$

Equation (2.18) depicts the natural convection behaviour which is occurred during the heat of a horizontal layer which creates a convection cells at the end of the process.

There are many factors that affect the diffusion rate such as the mass of molecules, temperature, the solubility of the material, the surface area, the thickness of the plasma membranes and density. Let us discuss each factor starting from the molecule mass, if the mass of the molecules is big, then the diffusion rate will be low. The next factor is temperature, due to the high temperature the kinetic energy of molecules increases the consequence of which is the increased diffusion rate. The third factor that changes the diffusion rate is the solubility of the material. Materials that can easily pass through the cell membranes like fat-soluble and non-polar materials increase the rate of the diffusion while other materials will decrease the diffusion rate. The next factors are the surface area and the thickness of the plasma membranes. The former affects in the way that when the surface area is higher then the diffusion rate will be higher, too. That shows the direct proportion between the diffusion rate

as well as the surface area. This is due to the fact that the higher surface area allows molecules pass to the other sides more easily. But, the latter describes the opposite proportion between the thickness and the diffusion rate: the higher the thickness provides, the less is the diffusion rate, because of the larger distance which results in more resistance to the molecules. The diffusion rate depends on the distance that substance must travel: the higher the thickness, the slower substance diffuses. Another factor that affects the diffusion rate is the density of the medium. The diffusion rate is higher when the density is smaller, and the diffusion rate is smaller when the density is higher. This is due to the fact that less density of the medium will ensure less resistance in movement of the molecules through the medium. One of the great examples is dehydration which leads to a shortage of water in the organism. Because of the deficiency in water, when the cytoplasm density increases then the diffusion rate decreases [66].

In this thesis work we will consider the density-dependent diffusion function. The examples of such functions are the followings [31]

$$D_1 - D_2 \tanh(au), \quad D_1 - \frac{D_2 u^n}{a^n + u^n}, \tag{2.19}$$

where D_1, D_2, a, n are parameters that satisfies next conditions: $D_1 \geq D_2, n \geq 1, a > 0$, and u is the cell density. The parameter n shows how considerably the diffusion function reduces while the parameter a identifies the cell density u which ensures the movement at half maximum rate. Also, D_1 and D_2 indicate the diapason of the diffusion function.

The second diffusion function is used in the analysis part of this work. Based on the paper of Stepien et al. [59] and Kashkynbayev et al. [31], we decided to examine diffusion function that satisfies the next conditions:

- $D(u)$ is a continuous and differentiable function;

- $D(u)$ is a positive and decreasing function for $u \geq 0$;

2.6 Growth functions

Despite the fact that almost all continuous, deterministic, cell-population based cancer models follow intrinsic tumor growth functions, it is not well established as to which intrinsic growth function should be used when a new mathematical model is being built. The most commonly used intrinsic growth functions are exponential and logistics growth functions, power Law functions, von Bertalanffy growth functions, and Gompertz growth function [14, 27]. The growth function is selected based on the cancer type as well as the environment of the tumor (for instance, in mice or rats, in vivo or in humans).

There are many researchers who compared growth functions with one another. The work written by Aroesty et al. is one of the earliest published works in this field. They analyzed which growth function best fits tumor data, the Gompertz or logistics functions. Instead of using any analytical or numerical methods to compare these growth functions, they only did work by listing the theoretical characteristics, similarities between logistics and Gompertz models. As a result, no analysis of the fitting process were given. Another paper was done by Hart et al.[27] in 1988 who compared four growth functions such as exponential, logistics, Gompertz and power growth law (exponent = 0.5) models in breast cancer. The authors used large-scale mammography screening data in order to derive the growth rate of breast cancer. They concluded that the best function that describes the growth of breast cancer is power law growth, and that other considered functions are inconsistent for this data type. Another study done by Zheng et al. [74] compares exponential and biexponential growth functions of lung cancer where the latter approximates the growth of the tumor with two different growth rates. This study identifies that the biexponential

model more accurately describes all tested cases in comparison with the exponential model. According to de Pillis [14], von Bertalanffy and logistics growth functions are well fit with the experimental data, which is shown via using a least-squares residual comparison method. In the paper, four different growth functions were considered and examined for case where human melanoma was grown in mice. In the same way the growth of bacteria were also studied and examined through different growth functions. In 2004, Lopez et al. considered nine different growth functions and two different data sets and they concluded that the best functions that describe the bacterial growth rate were three phase-linear, Baranyi, Richards and Weibull growth models. It must be noted that there was not shown any direct comparison processes of the fitting results.

Let us discuss briefly each of earlier mentioned intrinsic growth functions. The first application of mathematics was conducted by Thomas Malthus in 1798 and he created a model by using exponential growth law [68]. This Malthus model can be used in estimating the world population even if the model is unrealistic in fact [45]. It is a special case of power law growth function which is at the same time the simplest growth model that is given by the next equation

$$\frac{du}{dt} = ru \tag{2.20}$$

where u is the cell population, t represents a time and r is an intrinsic growth rate. The power law growth model is

$$\frac{du}{dt} = ru^{\alpha} \tag{2.21}$$

where α is a parameter that should be fitted by the data.

The next logistics growth model was proposed by a Belgian mathematician Pierre-

Francois Verhulst in 1838 [67], which is given in the form of

$$\frac{du}{dt} = ru\left(1 - \frac{u}{u_m}\right), \quad u_m \text{ - carrying capacity} \tag{2.22}$$

that looks very similar to the exponential model at low populations. One can see from the logistics model that it incorporates the carrying capacity.

The next model is von Bertalanffy growth model which also has a carrying capacity in the equation

$$\frac{du}{dt} = r(u_m - u) \tag{2.23}$$

and Gompertz growth function is given as the following

$$\frac{du}{dt} = ru\ln\left(\frac{u_m}{u}\right). \tag{2.24}$$

In recent years Gompertz model is also widely used in many researches and this can be viewed in works of Laird and McCredie. The former analyzed a tumor cell proliferation model which explains well the growth of a tumor. She figured out that the growth of a tumor slows down as time increases (note that the growth function is the Gompertzian function). Also, by using the least square methods she estimated the time as well as parameters. After analyzing 12 different tumors in rats, rabbits and mice, Laird [37, 38] concluded that Gompertz model describes tumor well. They also represented that the growth of organisms, whose growth range is above 10000-fold, as the guinea pig could be demonstrated by Gompertz function. While the latter, McCredie et al. [43], suggest that Gompertz function shows a better growth curves compared to the exponential function. Therefore, contributions of Laird and McCredie serve as the foundations for the mathematical oncology with using Gompertzian function for the real tumor growth situations [35, 36, 43]. Another research

paper written by Miljenko Marusic [42] well depicts how the data fits with Gompertz model and logistics model. The author used least square method to fit the model curve and compared it with the tumor data obtained via 45 measurements of volumes for the duration of 60 days. Further, he came to a conclusion that the Gompertz model accurately fits the data in comparison to models with other growth functions.

Gompertz function is also widely used as a growth curve for both biological and economic occurrences in 1932 by Winsor [72]. The study of Larry Norton [48] published in 1988 states that an experimental and clinical data are well fitted by the Gompertz equation which also reveals the mechanisms of growth regulation in animal and human cancers. Moreover, when it was used to relate tumors size to its regression rate in regards to therapy, the equation has helped to design successful clinical experiments.

2.7 Nelder-Mead algorithm

The numerical simulations were done by a simplex-based direct search Nelder-Mead method implemented in *fminsearch* function of Matlab program [16]. Nelder-Mead simplex method was introduced by Nelder and Mead in 1965 [47]. This method helps to minimize a function with n variables via interchanging the vertex by another point which is more closely located to the local minimum. After 10 years of this novelty, a significant research on this field was done by D.M. Olsson and L.S. Nelson who considered six minimization problems taken from Technometrics of May 1973 edition [49]. Their process was lasting for over two years and at the end they came to a conclusion that Nelder-Mead simplex method is capable to handle with different optimization problems without any modifications particularized to the current problem.

This algorithm goes though k-iterations which starts by sampling $n+1$ time values, which are denoted as follows

$$x_1,\ x_2,\ x_3,\ ...,\ x_{n+1}.$$

All these time values are sorted in ascending order by the values of the target function $f(x)$

$$f(x_1) \leq f(x_2) \leq f(x_3) \leq ... \leq f(x_{n+1}). \tag{2.25}$$

The point with i^{th} lowest value of the target function at the k^{th} iteration is notated as x_i^k. Next, we define a simplex function

$$S_k =< x_1,\ x_2,\ x_3,\ ...,\ x_{n+1} >$$

with $x_1,\ x_2,\ x_3,\ ...,\ x_{n+1}$ vertices. So, this simplex transformations are controlled by four parameters as reflection, expansion, contraction and shrinkage and retrofitted till S_{k+1} closely converges to the local minimum. First step reflects the worst vertex x_l through the centroid of other vertices and computes the reflected vertex as

$$x_l = (1+\alpha)\bar{x} - \alpha x_{n+1} \tag{2.26}$$

where $\alpha = 1$ and $\bar{x}$ is the centroid

$$\bar{x} = \frac{1}{n}\sum_{i=1}^{n} x_i. \tag{2.27}$$

If the reflected vertex satisfies the next inequality

$$f(x_1) \leq f(x_l) < f(x_n), \tag{2.28}$$

then we move on to the next iteration with the simplex $S_k =< x_1,\ x_2,\ x_3,\ ...,\ x_n, x_l >$. But if the reflected vertex has lower value in comparison with x_1, $x_l < x_1$, then this means that x_l is the closest point to the local minimum and we continue the algorithm with the expansion step

$$x_e = \gamma x_l + (1 - \gamma)\bar{x} \tag{2.29}$$

where $\gamma = 2$. If the expansion vertex is $f(x_e) \leq f(x_1)$ and reflected vertex otherwise, then these vertexes accepted. However, if none of them are accepted, in case of $f(x_n) \leq f(x_e)$ or $f(x_n) \leq f(x_1)$, we calculate the contracted vertex by the next formula

$$x_c = \beta x_{l'} + (1 - \beta)\bar{x}, \tag{2.30}$$

where $\beta = \frac{1}{2}$ and $x_{l'} = \min(x_{n+1}, x_l)$. We continue the iteration if the next condition is satisfied $f(x_c) < f(n)$, however, if $f(x_c) \leq f(n)$, then we shrink the simplex by replacing each x_i with the midpoint of x_1 and x_i

$$x_{i(new)} = \frac{x_1 + x_i}{2}. \tag{2.31}$$

The algorithm finds a new simplex by rearranging the new x_i with respect to the value of the target function $f(x)$. The Nelder-Mead algorithm finds a simplex that converges to the local minimum and shrinks if it does not define a point which cannot move deeper to the local minimum. Despite of this, the algorithm has many stopping criteria of the process, but *fminsearch* process in Matlab program stops when the moved distance during the last iteration is less than the initial tolerance.

Chapter 3

Traveling wave analysis

3.1 Existence of traveling wave solutions

In this section, the analysis of existing traveling wave solutions is shown by using phase plane analysis.

In one-dimensional Cartesian coordinates equation (1.1) will take the following form

$$\begin{aligned}
\frac{\partial u}{\partial t} &= \nabla D\left(\frac{u}{u_m}\right)\nabla u + D\left(\frac{u}{u_m}\right)\nabla^2 u + \rho u \ln\left(\frac{u_m}{u+\alpha}\right) - sign(x) v_i \nabla \cdot u. \\
\frac{\partial u}{\partial t} &= D'\left(\frac{u}{u_m}\right)\cdot\frac{1}{u_m}\cdot\frac{\partial u}{\partial x}\nabla u + D\left(\frac{u}{u_m}\right)\nabla^2 + \rho u \ln\left(\frac{u_m}{u+\alpha}\right) - v_i \nabla u. \qquad (3.1) \\
\frac{\partial u}{\partial t} &= \frac{1}{u_m} D'\left(\frac{u}{u_m}\right)\left(\frac{\partial u}{\partial x}\right)^2 + D\left(\frac{u}{u_m}\right)\left(\frac{\partial u}{\partial x}\right)^2 + \rho u \ln\left(\frac{u_m}{u+\alpha}\right) - v_i \frac{\partial u}{\partial x}.
\end{aligned}$$

Let us multiply both sides of the last equation by $\frac{1}{\rho u_m}$, then we have

$$\frac{1}{\rho u_m}\frac{\partial u}{\partial t} = \frac{1}{\rho u_m} D\left(\frac{u}{u_m}\right)\frac{\partial^2 u}{\partial x^2} + \frac{1}{\rho u_m}\frac{1}{u_m} D'\left(\frac{u}{u_m}\right)\left(\frac{\partial u}{\partial x}\right)^2 - \frac{1}{\rho u_m} v_i \frac{\partial u}{\partial x} + \frac{1}{\rho u_m}\rho u \ln\left(\frac{u_m}{u+\alpha}\right).$$

which is the same as

$$\frac{\partial(\frac{u}{u_m})}{\partial(\rho t)} = D\left(\frac{u}{u_m}\right)\frac{\partial^2(\frac{u}{u_m})}{\partial\left(\sqrt{\rho}x\right)^2} + D'\left(\frac{u}{u_m}\right)\left(\frac{\partial(\frac{u}{u_m})}{\partial\left(\sqrt{\rho}x\right)}\right)^2 - \frac{v_i}{\sqrt{\rho}}\frac{\partial(\frac{u}{u_m})}{\partial\left(\sqrt{\rho}x\right)} + \frac{\rho}{\rho}\frac{u}{u_m}\ln\left(\frac{u_m}{u+\alpha}\right). \tag{3.2}$$

Also, in order to obtain the equivalent form of the equation (3.1), we substitute instead of

$$\rho t \mapsto t, \quad x\sqrt{\rho} \mapsto x, \quad \frac{u}{u_m} \mapsto u, \quad \frac{\alpha}{u_m} \mapsto \alpha, \tag{3.3}$$

and define a new parameter

$$p = \frac{v_i}{\sqrt{\rho}}. \tag{3.4}$$

Then we get

$$\frac{\partial u}{\partial t} = D(u)\frac{\partial^2 u}{\partial x^2} + D'(u)\left(\frac{\partial u}{\partial x}\right)^2 - p\frac{\partial u}{\partial x} + u\ln\left(\frac{1}{u+\alpha}\right), \tag{3.5}$$

which is equivalent to

$$\frac{\partial u}{\partial t} = D(u)\frac{\partial^2 u}{\partial x^2} + D'(u)\left(\frac{\partial u}{\partial x}\right)^2 - p\frac{\partial u}{\partial x} - u\ln(u+\alpha). \tag{3.6}$$

We are aimed to find a traveling wave solution of the equation (3.6) in the form of

$$u(x,t) = h(x-ct) := h(y), \tag{3.7}$$

where the speed of a traveling wave solution should be non-negative ($c \geq 0$) and the function $h(y)$ must be defined on $\mathbb{R}$ and should satisfy the next boundary conditions:

$$\lim_{y\to-\infty} h(y) = 1 \text{ and } \lim_{y\to\infty} h(y) = 0. \tag{3.8}$$

By substituting ansatz (3.7) into (3.6) and applying the chain rule, we obtain the following second-order ordinary differential equation with boundary conditions

$$D(h(y))h''(y) + (c-p)h'(y) + D'(h(y))(h'(y))^2 - h(y)\ln(h(y)+\alpha) = 0. \tag{3.9}$$

Due to the choice of function D, where D is a positive decreasing function, we have $D(h(y)) > 0$. Then by setting $k = dh/dk$ and dividing the equation (3.9) by $D(h(y))$ we arrive at the following system of first-order ordinary differential equations.

$$\begin{aligned} h' &= k, \\ k' &= -\frac{1}{D(h)}((c-p)k + D'(h)k^2 - h\ln(h+\alpha)). \end{aligned} \tag{3.10}$$

Now, let us find the fixed points of the system (3.10). When $k = 0 \implies h\ln(h+\alpha) = 0$. Then either $h = 0$ or $\ln(h+\alpha) = 0$, which leads to $h = 1-\alpha$. Let us consider three cases: $\alpha > 1$, $\alpha = 1$ and $\alpha < 1$. If $\alpha > 1$, then $h < 0$, which does not have a biological meaning. When $\alpha = 1$, then $h = 0$ which coincides with the first fixed point. So, we remain with the third case: $h > 0$ when $\alpha < 1$. Therefore, α should be in-between $(0, 1)$.

After finding the fixed points, we compute the Jacobian matrices by linearizing the system (3.10) around the equilibrium points

$$J = \begin{pmatrix} 0 & 1 \\ \frac{D'(h)((c-p)k+D'(h)k^2-h\ln(h+\alpha))}{D^2(h)} - \frac{D''(h)k^2-\ln(h+\alpha)-\frac{h}{h+\alpha}}{D(h)} & \frac{p-c}{D(h)} - \frac{2D'(h)k}{D(h)} \end{pmatrix}. \tag{3.11}$$

The Jacobian matrix at $(0, 0)$ is

$$J_1 := J(0,0) = \begin{pmatrix} 0 & 1 \\ \frac{\ln(\alpha)}{D(0)} & \frac{p-c}{D(0)} \end{pmatrix}. \tag{3.12}$$

Since $\alpha < 1$ $\det J_1 > 0$, $\mathrm{tr} J_1 = \frac{p-c}{D(0)}$. If we assume that $c > p$, then $\mathrm{tr} J_1 < 0$. Hence, it can be concluded that $(0,0)$ is a stable node or a stable spiral. Since oscillations are not possible in the tumor cell dynamics, we can say that $(0,0)$ is a stable node. So, in order to find the precise condition for c, we will rule out the negative value of a square root of J_1 eigenvalues

$$\lambda^2 - \frac{p-c}{D(0)}\lambda - \frac{\ln(\alpha)}{D(0)} = 0 \tag{3.13}$$

$$\lambda_{1,2} = \frac{(p-c) \pm \sqrt{(p-c)^2 + 4\ln(\alpha)D(0)}}{2D(0)}.$$

The value of a square root should be bigger or equal to zero, since, as we said earlier, oscillations are not possible in the tumor cell dynamics

$$(p-c)^2 + 4\ln(\alpha)D(0) \geq 0. \tag{3.14}$$

If we take the square root from both sides, then

$$(p-c) \geq \pm 2\sqrt{-\ln(\alpha)D(0)}. \tag{3.15}$$

Since $c > p$ the left hand side of the following inequality is negative, while the right hand side is positive. This is impossible, hence we will not consider this case

$$p - c \geq \ 2\sqrt{-\ln(\alpha)D(0)}. \tag{3.16}$$

The second case is with the minus sign

$$p - c \geq -2\sqrt{-\ln(\alpha)D(0)}, \tag{3.17}$$

which leads to

$$p + 2\sqrt{-\ln(\alpha)D(0)} \geq c. \tag{3.18}$$

Hence,

$$c_{min} = p + 2\sqrt{-\ln(\alpha)D(0)}. \tag{3.19}$$

The Jacobian matrix evaluated at $(1-\alpha, 0)$ is

$$J_2 := J(1-\alpha, 0) = \begin{pmatrix} 0 & 1 \\ \frac{1-\alpha}{D(1-\alpha)} & \frac{p-c}{D(1-\alpha)} \end{pmatrix}. \tag{3.20}$$

One can easily see that $\det J_2 = -\frac{1-\alpha}{D(1-\alpha)} < 0$, because of $D(1-\alpha) > 0$, thus $(1-\alpha, 0)$ is a saddle equilibrium point.

3.2 Phase plane analysis

In this section, we aim to prove the existence of a traveling wave solution under the condition (3.19) that satisfies

$$\lim_{y\to-\infty}(h,k) = (1,0) \text{ and } \lim_{y\to\infty}(h,k) = (0,0). \tag{3.21}$$

To prove this, we need to construct a heteroclinic orbit connecting the two steady-state solutions. To this end, we use phase plane analysis and construct a positively invariant region to trap the unstable orbit emanating from the saddle point $(1-\alpha, 0)$.

Lemma 1. *Let Ω be the open region bounded by the lines*

$$L_1 = \{(h,k) : 0 \leq h \leq 1-\alpha, k = 0\},$$
$$L_2 = \{(h,k) : 0 \leq h \leq 1-\alpha, k = \lambda_1 h\},$$
$$L_3 = \{(h,k) : h = 1-\alpha, \lambda_1 \leq k \leq 0\}.$$

Then Ω is positively invariant region.

Proof. Consider the line

$$L_1 = \{(h,k) : 0 \leq h \leq 1-\alpha, k = 0\}. \tag{3.22}$$

Note that the horizontal line $k = 0$ is h nullcline of the system (3.10). Moreover, on L_1 we have

$$k' = \frac{h\ln(h+\alpha)}{D(h)}. \tag{3.23}$$

In order to find the direction fields on the line L_1, let us choose $h = \frac{1-\alpha}{2}$, then

$$k' = \frac{1-\alpha}{2}\ln\left(\frac{1+\alpha}{2}\right)\frac{1}{D(1-\alpha)}.$$

This implies that $k' < 0$ on L_1 since $\ln(h+\alpha) < 0$ for $h \in [0, 1-\alpha]$ and $\alpha \in (0,1)$. Thus, the direction fields on the line L_1 is in the negative k direction.

Next, let us consider the line

$$L_2 = \{(h,k) : 0 \leq h \leq 1-\alpha, k = \lambda_1 h\}, \tag{3.24}$$

where λ_1 is the more negative eigenvalue ($\lambda_1 < 0$) of J_1 , i.e.,

$$\lambda_1 = \frac{(p-c) - \sqrt{(p-c)^2 + 4D(0)\ln(\alpha)}}{2D(0)}. \tag{3.25}$$

Since our diffusion function is $D(u) = D_1 - \frac{D_2 u^n}{a^n + u^n}$, $D(0) = D_1$, then λ_1 obtains the next form

$$\lambda_1 = \frac{(p-c) - \sqrt{(p-c)^2 + 4D_1\ln(\alpha)}}{2D_1}, \tag{3.26}$$

$$2D_1\lambda_1 = (p-c) - \sqrt{(p-c)^2 + 4D_1\ln(\alpha)}, \tag{3.27}$$

$$2D_1\lambda_1 - (p-c) = -\sqrt{(p-c)^2 + 4D_1\ln(\alpha)}. \tag{3.28}$$

We square both sides of (3.28), then we have the following

$$4D_1^2\lambda_1^2 - 4D_1\lambda_1(p-c) + (p-c)^2 = (p-c)^2 + 4D_1\ln(\alpha), \tag{3.29}$$

$$D_1\lambda_1^2 - \lambda_1(p-c) = \ln(\alpha). \tag{3.30}$$

Therefore, λ_1 satisfies the following equation

$$\lambda_1(c-p) = \ln(\alpha) - D_1\lambda_1^2. \tag{3.31}$$

The normal vector to the line L_2 in the positive k direction is given by $(-\lambda_1, 1)$. Along L_2 the system (3.10) is equivalent to

$$\begin{aligned} h' &= \lambda_1 h, \\ k' &= -\frac{1}{D(h)}((c-p)\lambda_1 h + D'(h)(\lambda_1 h)^2 - h\ln(h+\alpha)). \end{aligned} \tag{3.32}$$

Thus, the inner product between the normal vector to L_2 and the vector field gives

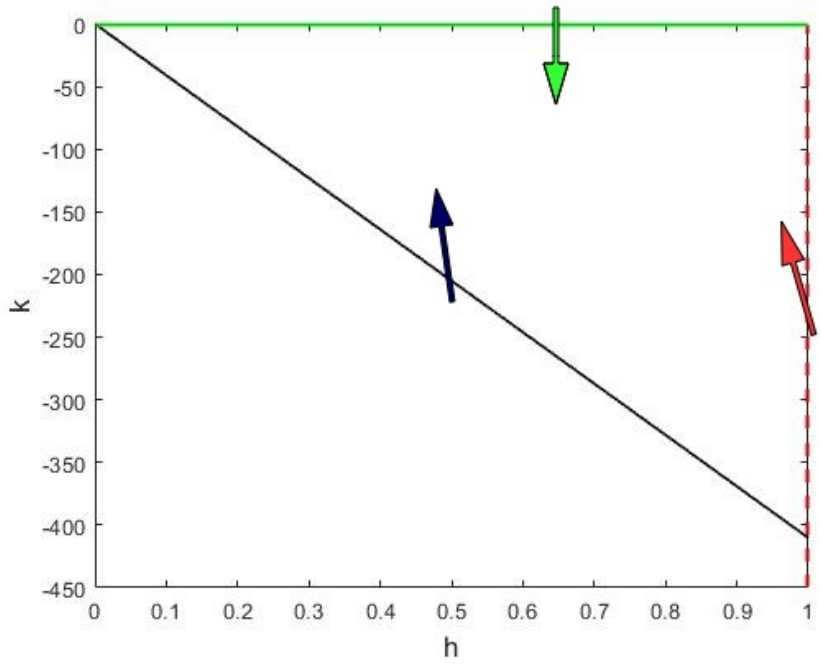

Figure 3-1: Triangular region with estimated parameters of Table 4.1. The green line is L_1 (3.22) the vertical nullcline, the dark blue line is L_2 (3.24) corresponding to the eigenvector of linearized system at (0, 0) and the dashed red line is L_3 (3.36). The arrows show direction of flow.

us

$$\begin{aligned}(-\lambda_1, 1)\cdot(h', k') &= -\lambda_1^2 h - \frac{1}{D(h)}((c-p)\lambda_1 h + D'(h)(\lambda_1 h)^2 - h\ln(h+\alpha)) \\ &= -\frac{h}{D(h)}\left(\lambda_1^2 D(h) + (c-p)\lambda_1 + D'(h)\lambda_1^2 h - \ln(h+\alpha)\right).\end{aligned} \tag{3.33}$$

Due to the relation (3.31) we have

$$\begin{aligned}(-\lambda_1, 1)\cdot(h', k') &= -\frac{h}{D(h)}\left(\lambda_1^2 D(h) + (c-p)\lambda_1 + D'(h)\lambda_1^2 h - \ln(h+\alpha)\right) \\ &= -\frac{h}{D(h)}\left(\lambda_1^2 D(h) + \ln(\alpha) - D_1\lambda_1^2 + D'(h)\lambda_1^2 h - \ln(h+\alpha)\right) \\ &= -\frac{h}{D(h)}\left(\lambda_1^2[D(h) - D_1 + D'(h)h] + \ln(\alpha) - \ln(h+\alpha)\right).\end{aligned} \tag{3.34}$$

By monotonicity of the diffusion function we have $0 < D(h) < D(0)$ and $D'(h) < 0$

for $h \in [0, 1-\alpha]$. Hence, we have $-\frac{h}{D(h)} \leq 0$ and $\lambda_1^2[D(h) - D_1 + D'(h)h] \leq 0$. Since $f(h) = \ln(\alpha) - \ln(h+\alpha)$ is a decreasing function, we can conclude that $f(h) \leq 0$ in the interval of $0 \leq h \leq 1-\alpha$. Thus, the inner product satisfies

$$(-\lambda_1, 1) \cdot (h', k') \geq 0. \tag{3.35}$$

For this reason the angle between the direction fields and the normal vector is an acute angle. The flow across the line L_2 is in the positive k.

As the third edge of a triangular region the next line can be defined:

$$L_3 = \{(h, k) : h = 1-\alpha, \lambda_1 \leq k \leq 0\}. \tag{3.36}$$

It is easy to notice that the flow across this line is in the negative h direction. As a proof of this let us take, for instance, $h = 1-\alpha$ and $k = \frac{\lambda_1}{2}$. Then $h' = k = \frac{\lambda_1}{2} < 0$. So, this proves the provided statement above. Thus, the triangular region Ω bounded by L_1, L_2 and L_3 is positively invariant. □

Thus, we summarize the discussion above in the following theorem.

Theorem 2. *There exists a traveling wave solution in the form (3.7) of density-dependent reaction diffusion equation (3.6) that satisfies the boundary conditions* $u(x,t) \to 1$ *as* $x \to -\infty$ *and* $u(x,t) \to 0$ *as* $x \to \infty$ *with* $0 < u(x,t) < 1$*, whose orbit connects the steady states* $u = 0$ *and* $u = 1-\alpha$ *if and only if (3.19) is satisfied.*

Proof. We first show that the unstable manifold of the saddle point $(h, k) = (1-\alpha, 0)$ has nonempty intersection with Ω for all time. Consider k-isoclines which satisfy

$$-\frac{1}{D(h)}((c-p)k + D'(h)k^2 - h\ln(h+\alpha)) = 0,$$

$$D'(h)k^2 + (c-p)k - h\ln(h+\alpha) = 0. \tag{3.37}$$

Then the solutions are

$$k_+(h) = \frac{-(c-p) + \sqrt{(c-p)^2 + 4D'(h)h\ln(h+\alpha)}}{2D'(h)}, \tag{3.38}$$

$$k_-(h) = \frac{-(c-p) - \sqrt{(c-p)^2 + 4D'(h)h\ln(h+\alpha)}}{2D'(h)}. \tag{3.39}$$

Since $c > p$ the slope of the k_+ isocline at $h = 1-\alpha$ is

$$\begin{aligned} k'_+(h) =& \frac{D''(h)h\ln(h+\alpha) + \ln(h+\alpha)D'(h) + \frac{D'(h)h}{h+\alpha}}{D'(h)\sqrt{(c-p)^2 + 4D'(h)h\ln(h+\alpha)}} \\ & - \frac{D''(h)\big(p-c+\sqrt{(c-p)^2 + 4D'(h)h\ln(h+\alpha)}\big)}{2(D'(h))^2}, \end{aligned}$$

$$k'_+(1-\alpha) = \frac{4(D'(h))^2 h}{c-p} > 0, \tag{3.40}$$

and the eigenvector of the linearized system corresponding to the positive eigenvalue at the saddle point $(1-\alpha, 0)$ is

$$\eta = \left(1, \frac{1}{2}\left(\frac{p-c}{D(1-\alpha)} + \frac{\sqrt{(p-c)^2 + 4(1-\alpha)D(1-\alpha)}}{D(1-\alpha)}\right)\right)^T. \tag{3.41}$$

It is easy to see that

$$\begin{aligned} \sqrt{\frac{(p-c)^2}{D^2(1-\alpha)} + \frac{4(1-\alpha)}{D(1-\alpha)}} &< \sqrt{\frac{(p-c)^2}{D^2(1-\alpha)} + \frac{4(1-\alpha)}{D(1-\alpha)} + \frac{2^2(1-\alpha)^2}{(p-c)^2}} \\ &= \frac{p-c}{D(1-\alpha)} + \frac{2(1-\alpha)}{p-c}. \end{aligned} \tag{3.42}$$

Consequently,

$$\frac{1}{2}\left(\frac{p-c}{D(1-\alpha)}+\frac{\sqrt{(p-c)^2+4(1-\alpha)D(1-\alpha)}}{D(1-\alpha)}\right)<\frac{p-c}{D(1-\alpha)}+\frac{1-\alpha}{p-c}$$
$$=-\frac{c-p}{D(1-\alpha)}-\frac{1-\alpha}{c-p}<k'_+(1-\alpha). \tag{3.43}$$

From the analysis above we conclude that the slope of the eigenvector η is less than $k'_+(1-\alpha)$. Also, the trajectory that leaves $(1-\alpha,0)$ in the negative k direction has the tangent vector η at $(1-\alpha,0)$. Hence, these trajectories leave $(1-\alpha,0)$ above k_+. Then, we know that near $h=1-\alpha$, $k_+(h)$ is contained in Ω and the direction fields on the curve k_+ is horizontal in the negative h direction. Thus, the unstable manifold of the saddle at $(1-\alpha,0)$ remains in the region Ω for all time, and in addition to that, the ω-limit set of the corresponding orbit is also in Ω. Since $h'=k\leq 0$ within Ω and there is no any steady states in this positively invariant region, it can be concluded by the Poincare–Bendixson theorem that there are no periodic orbits in the interior of Ω. The ω-limit set must be contained in the boundary of Ω, and therefore, the ω-limit set is (0, 0). Hence, there exists a heteroclinic orbit connecting the equilibrium points $(h,k)=(0,0)$ and $(h,k)=(1-\alpha,0)$ when the minimum wave speed c_{min} is satisfied, which implies that a traveling wave solution exists. □

3.3 Wave profile analysis

Wave profile analysis was done based on the expansion method for singular perturbed problems in [28].

The trajectories defined by equation (3.9) in the phase plane are given by

$$\frac{dk}{dh}=\frac{-\frac{1}{D(h)}((c-p)k+D'(h)k^2-h\ln(h+\alpha))}{k}. \tag{3.44}$$

If we let

$$k \equiv \frac{1}{c}\eta \tag{3.45}$$

Equation (3.44) may be rewritten

$$\frac{1}{c^2}\eta\frac{d\eta}{dh} = -\frac{1}{D(h)}\left((c-p)\frac{1}{c}\eta + D'(h)\left(\frac{1}{c}\eta\right)^2 - h\ln(h+\alpha)\right) \tag{3.46}$$

If we set

$$\varepsilon \equiv \frac{1}{c} \tag{3.47}$$

Then we can get

$$\varepsilon^2\eta\frac{d\eta}{dh} = -\frac{1}{D(h)}\left(\eta - \varepsilon p\eta + \varepsilon^2 D'(h)\eta^2 - h\ln(h+\alpha))\right) \tag{3.48}$$

The equation (3.48) is the singularly perturbed equation and the usual perturbation theory is not applicable. Thus, we ignore all terms which are higher than the first order in ε

$$\eta - \varepsilon p\eta - h\ln(h+\alpha)) = 0 \tag{3.49}$$

The expansion method can be applied to the singular root by posing a power series in ε which starts with an ε^{-1} term instead of the usual ε^0.

$$\eta(h,\varepsilon) = \varepsilon^{-1}\eta_{-1}(h) + \eta_0(h) + \varepsilon\eta_1(h) + \varepsilon^2\eta_2(h) + ... \tag{3.50}$$

If we plug this expression into equation (3.49) and match powers of ε, we get

$$(1-\varepsilon p)(\varepsilon^{-1}\eta_{-1}(h) + \eta_0(h) + \varepsilon\eta_1(h) + \varepsilon^2\eta_2(h) + ...) - h\ln(h+\alpha)) = 0 \tag{3.51}$$

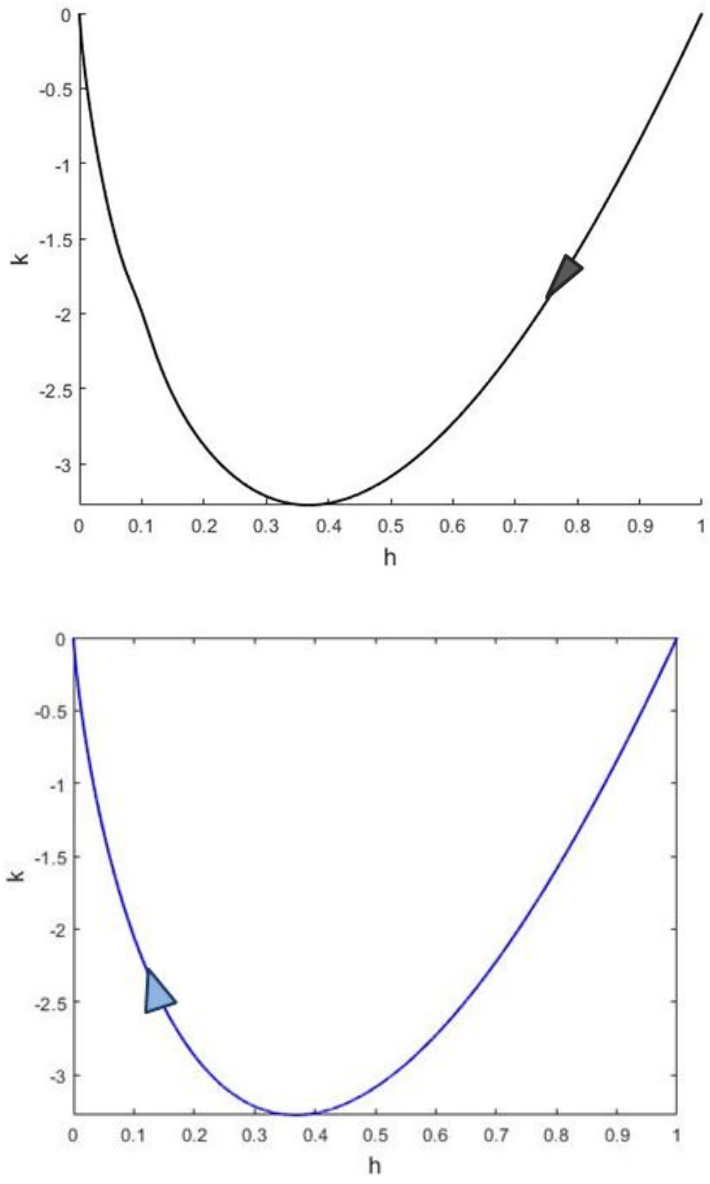

Figure 3-2: A black curve represents the heteroclinic connection of the original system (3.10) with estimated parameters of Table 4.1. A blue curve represents the approximated heteroclinic connection of (3.54) with optimal parameters of Table 4.1

ε^{-1} :

$$\eta_{-1}(h) = 0. \tag{3.52}$$

ε^0 :

$$\eta_0(h) = h\ln(h+\alpha),$$

ε^1 :

$$\eta_1(h) = p\eta_0(h) = ph\ln(h+\alpha).$$

ε^2 :

$$\eta_2(h) = p\eta_1(h) = p^2 h\ln(h+\alpha).$$

and so on. We can easily chain our way up this sequence of equations. It follows that the heteroclinic connection takes the form

$$\begin{aligned}\eta(h) &= \varepsilon^{-1}\eta_{-1}(h) + \eta_0(h) + \varepsilon\eta_1(h) + \varepsilon^2\eta_2(h) + ... \\ &= h\ln(h+\alpha) + \varepsilon ph\ln(h+\alpha) + \varepsilon^2 p^2 h\ln(h+\alpha) + ...\end{aligned} \tag{3.53}$$

This can also be written, in terms of the original h and k as

$$k(h) = \varepsilon h\ln(h+\alpha) + \varepsilon^2 ph\ln(h+\alpha) + \varepsilon^3 p^2 h\ln(h+\alpha) + .. \tag{3.54}$$

Chapter 4

Numerical simulations

This section demonstrates the computational results of the model and compares them with the experimental data obtained by Stein et al [58]. While Stein et al. considers two types of human astrocytoma cell line U87, to be precisely, they are U87WT wild-type receptor and U87ΔEGFR - the most common mutation of the Epidermal Growth Factor Receptor gene, we take into consideration only the first type of cell line. The reason of this is to show that the model with Gompertz growth function is at least that effective even for the strongest migratory cells as for other models [31, 58, 59]. By using the MATLAB function - GRABIT, which collects the data points from an image, the experimental data was obtained.

The tumor cells can move over a large spatial domain, but due to the boundary conditions the tumor does not exist at the boundaries, which mathematically means that when $x = \pm 1$ cm then $u(x,t) = 0$. Since the tumor is symmetric and because of these boundary conditions it is sufficient for us to consider only half of the domain from $x = 0$ to $x = 1$. In the simulation process Stein et al. considered the case when the initial cell density was zero since they do not model the core cells of the tumor in their equation. While as it is in models of Stepien et al. and Kashkynbayev et al., our modified Gompertzian model also considers all the tumor cells. As it was assumed

in Stein et al. work, we also assume that the cell density is 95% of $u_m = 4.2 \times 10^8$ cells/cm^3 for the 210 μm initial core tumor radius and zero elsewhere.

Our model has seven parameters which are $D_1, D_2, a, n, \rho, v_i, \alpha$. Based on the Stein et al. paper, the estimated ranges for some of the parameters were obtained. Specifically, D_1 - the diffusion where the cell density is small - is assumed to be in the order of 10^{-4}, while the growth rate ρ should be in range of $(0, 1)$. The value of v_i is estimated to be between $(0, 0.02)$. However, the assumed range for the next parameters a, n and α are not available, due to the non-existence of precedent in [58] to compare with.

Following the research paper by Stepien et al., the error function that we aimed to minimize is the same as in [31, 59] and has the following form

$$Error = \left(\sum_{i=1}^{M} \frac{|u_{data}(3, x_i) - u_{model}(3, x_i)|}{u_{data}(3, x_i)} + \sum_{t=1}^{N} \frac{|r_{data}(t) - r_{model}(t)|}{r_{data}(t)} \right) \cdot \frac{1}{N + M - (q + 1)}, \tag{4.1}$$

where $N = 7$ - the total number of days for which there exist invasive radii data, $M = 17$ - the total number of cell densities for the third day of experiment and $q = 7$ - the number of parameters that were optimized. The first sum of the error function compares the experimental data points x_i of the cell density at day 3 and the model data points, while the second sum compares the invasive radii of the experimental data and the model.

4.1 Parameter estimation

The parameters D_1, D_2, a, n, ρ, v_i and α were tested for sensitivity and each of them was in the biological relevant range ($D_1 \geq D_2, n \geq 1, a > 0$). In order to do a parameter sensitivity analysis of one parameter, the selected parameter varied

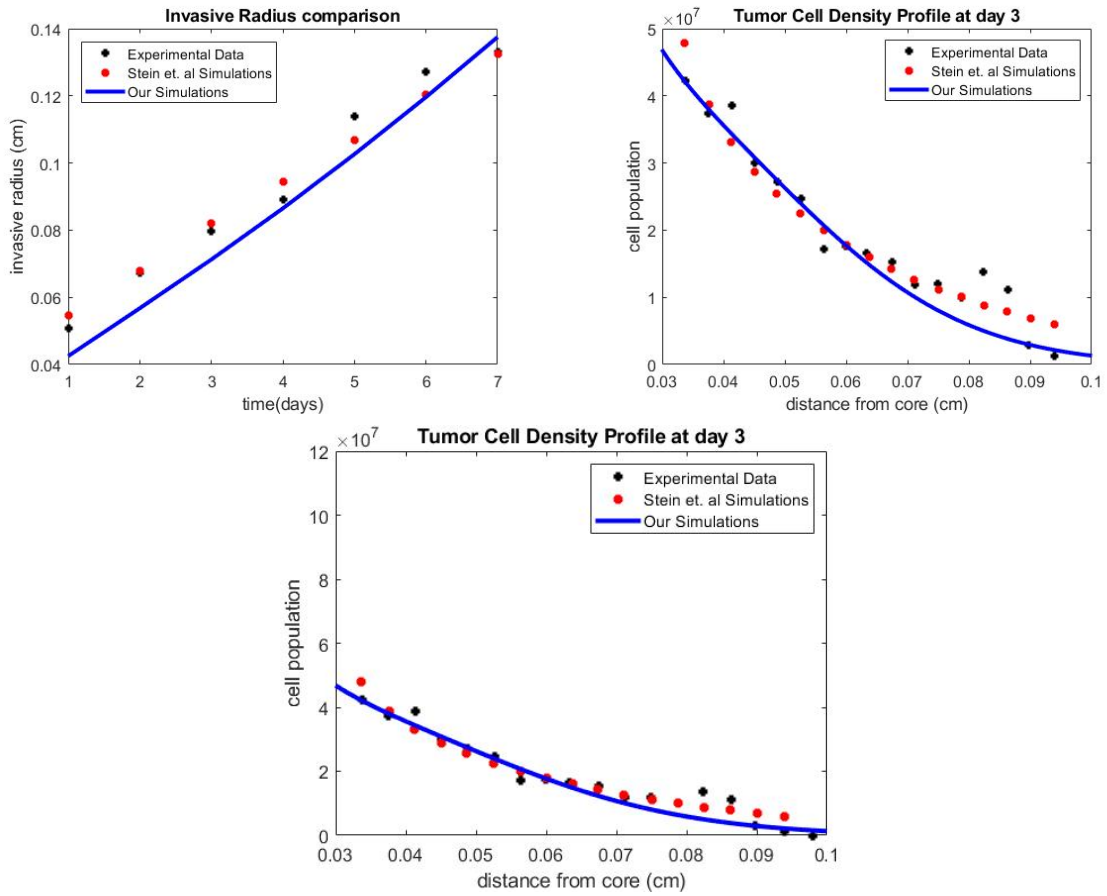

Figure 4-1: Numerical solution of the density-dependent diffusion glioblastoma model (1.1) with optimized parameter values in Table 4.1 compared to experimental data from Stein et al. [58] and their simulations.

whereas all other parameters were taken as constants. The sensitivity analysis is used to perform optimization that guides us how to choose the parameters to minimize the error function. As a result, some parameters can be more sensitive than others. Sensitivity of parameters describes the change of the error function depending on one parameter.

So, we run Matlab code, fixed all parameters except one, and then tested different values of that excepted parameter to see how the total error changes. We performed the same simulation process for all seven parameters and analyze them with each other. Then defined which one is more (less) sensitive in comparison with other parameters. This simulation showed that D_1, a, n, D_2 and ρ are more sensitive than v_i, α since the total error more depends on the values of that first parameters.

By minimizing (4.1) and by applying *fminsearch* MATLAB function the optimal parameters were estimated. Different initial parameters were chosen in order to find the estimated parameters that better minimize the error function compared to others.

Parameter	Initial condition	Optimal value
D_1	1.3685×10^{-4} cm^2/day	1.3685×10^{-4} cm^2/day
D_2	1.3645×10^{-4} cm^2/day	1.3642×10^{-4} cm^2/day
a	0.0972 cells/cm^2	0.1002 cells/cm^2
n	4.7966	7.4941
ρ	0.1421 /day	0.1442 /day
v_i	8.7174×10^{-11} cm/day	6.4526×10^{-11} cm/day
α	1.0165×10^{-10}	1.0048×10^{-10}
Total error: 0.2216		

Table 4.1: The parameter estimations of the model obtained by numerical computations.

Chapter 5

Discussion

We have analyzed density-dependent reaction-diffusion equation with modified Gompertz growth function. The considered diffusion function is differentiable positive decreasing function because of the experiment done by Stein et al. [58]. A Gompertzian growth function is modified and the following changes were made: (a) coefficients of the classical Gompertz growth function is assumed to be equal to 1; (b) to have a biological meaning and to prevent numerical errors some value α was added to the part of $\ln(u)$ that assures the maximum growth rate. By phase plane analysis and numerical simulations we have found a condition for the existence of traveling wave solutions which states that if the minimum wave speed (5) is satisfied then the traveling wave solution exists.

The model itself consists of three terms such as density-dependent diffusion, taxis and a growth function. The following diffusion function was used in the model

$$D(u) = D_1 - \frac{D_2 u^n}{a^n + u^n}, \tag{5.1}$$

which is inversely proportional to the cell density. Due to cell–cell mutual interference in high density regions and cell–cell adhesion in medium density regions, the diffusion

is large where the cell density is small and the diffusion is small where the cell density is large.

Via numerical simulations we have found optimal parameters for the Gompertzian GBM model. So the findings depict that $D_1 > D_2$ as needed, despite of the fact they are both close to zero. In comparison to [31, 59] the best value of the degree at which cells migrate away from the core, v_i, is smaller for Gompertzian model than for logistics and Bernoulli's models. As opposed to previous studies, our model has an additional parameter α which prevents numerical errors and ensures biological meaning for the model. So the numerical results show that the optimal parameter for α is a very small number close to 0.

It can be concluded from Figure 4-1 that there is inconsiderable discrepancy between the experimental data and our simulation which means that the Gompertzian model well fits the experimental data. The figures well depict that our one-dimensional model as accurate as a three-dimensional Stein et al.'s model. This was concluded based on the location of cell densities which indicates the victorious successful fixation of the tumor core cells and migratory cells. In addition to that, the total error for Gompertzian GBM model obtained via numerical simulations was bigger than in [59] case, which is 0.21, and less than in [31], that is 0.2337.

By the wave profile analysis we have found the approximated heteroclinic connection, which is actually the same as the connection obtained via numerical simulations. As ε we chose the reciprocal of the minimum wave speed, where $c_{min} = 0.1123$ cm/day. This describes the accuracy of the model as well as numerical results.

Chapter 6

Conclusions and future directions

6.1 Conclusions

The model introduced by [31, 59] simplifies the modeling of glioblastoma multiforme tumor type which also makes the numerical computations faster and the analysis simpler. The phase plane analysis as well as wave profile analysis were performed, and the condition of minimum wave speed is found. Existence of invariant triangular region was proved, and by applying Poincare-Bendixson theorem it was shown that there is not any periodic orbits in this region. Also, these analysis coincides with one another that shows the correctness of analysis.

In numerical simulations we used the Nelder-Mead simplex method to find optimal parameters of the model through which the minimum wave speed is calculated, which is approximately 0.1123 cm/day. Additionally, by using these optimal parameters the heteroclinic connections in the wave profile analysis sections are drawn.

By taking into account all research work that was presented above and also by comparing those results with other research papers, it can be concluded that the Gompertzian function well fits the experimental data as logistics and Bernoulli do.

6.2 Future directions

Future studies of glioblastoma growth can be improved by replacing the diffusion Laplace part by the p-Laplacian or the porous medium fast diffusion operator and also by considering another growth function as von Bertalanffy with different μ-degrees. Another possible direction is to consider two- or three-dimensional models with multiple cell populations. Additionally, stochastic case can be considered too.

The numerical part can be improved by using finite element methods and also, by plotting the figures in three dimensional case. Another way of improving the numerical part can be achieved by plotting the figures in polar coordinates.

Bibliography

[1] Cory Adamson, Okezie O Kanu, Ankit I Mehta, Chunhui Di, Ningjing Lin, Austin K Mattox, and Darell D Bigner. Glioblastoma multiforme: a review of where we have been and where we are going. *Expert Opinion on Investigational Drugs*, 18(8):1061–1083, 2009. PMID: 19555299.

[2] Kenneth D Aldape, M Fatih Okcu, Melissa L Bondy, and Margaret Wrensch. Molecular epidemiology of glioblastoma. *The Cancer Journal*, 9(2):99–106, 2003.

[3] Daniel Bernoulli. Essai d'une nouvelle analyse de la mortalité causée par la petite vérole, et des avantages de l'inoculation pour la prévenir. *Histoire de l'Acad., Roy. Sci.(Paris) avec Mem*, pages 1–45, 1760.

[4] Juliette Bouhours and Grégoire Nadin. A variational approach to reaction diffusion equations with forced speed in dimension 1. *arXiv preprint arXiv:1310.3689*, 2013.

[5] Patricia K Burgess, Paul M Kulesa, James D Murray, and Ellsworth C Alvord Jr. The interaction of growth rates and diffusion coefficients in a three-dimensional mathematical model of gliomas. *Journal of Neuropathology & Experimental Neurology*, 56(6):704–713, 1997.

[6] Helen M Byrne and Mark AJ Chaplain. Modelling the role of cell-cell adhesion in the growth and development of carcinomas. *Mathematical and Computer Modelling*, 24(12):1–17, 1996.

[7] Anna Q Cai, Kerry A Landman, and Barry D Hughes. Multi-scale modeling of a wound-healing cell migration assay. *Journal of Theoretical Biology*, 245(3):576–594, 2007.

[8] Jose Canosa. On a nonlinear diffusion equation describing population growth. *IBM Journal of Research and Development*, 17(4):307–313, 1973.

[9] Vincent P Collins. Observation on growth rates of human tumors. *Am J Roentgenol*, 76:988–1000, 1956.

[10] Edward Lansing Cussler and Edward Lansing Cussler. *Diffusion: mass transfer in fluid systems*. Cambridge university press, 2009.

[11] D Cvetkoivč-Dožič, M Skender-Gazibara, and S Dožič. Morphological and molecular features of diffuse infiltrating astrocytoma. *Arch Oncol*, 12:38–39, 2004.

[12] Sunit Das, Maya Srikanth, and John A Kessler. Cancer stem cells and glioma. *Nature clinical practice Neurology*, 4(8):427–435, 2008.

[13] Lisette G De Pillis and Ami Radunskaya. A mathematical tumor model with immune resistance and drug therapy: an optimal control approach. *Computational and Mathematical Methods in Medicine*, 3(2):79–100, 2001.

[14] Lisette G de Pillis and Ami E Radunskaya. Some promising approaches to tumor-immune modeling. *Contemporary Mathematics*, 410:89, 2006.

[15] Syreeta DeCordova, Abhishek Shastri, Anthony G Tsolaki, Hadida Yasmin, Lukas Klein, Shiv K Singh, and Uday Kishore. Molecular heterogeneity and immunosuppressive microenvironment in glioblastoma. *Frontiers in Immunology*, 11:1402, 2020.

[16] JE Dennis and Daniel J Woods. Optimization on microcomputers: The nelder-mead simplex algorithm. *New computing environments: microcomputers in large-scale computing*, 11:6–122, 1987.

[17] Odo Diekmann. Dynamics in bio-mathematical perspective. *Math. Comput. Sci. II*, 4:23–50, 1986.

[18] Steffen Erik Eikenberry, Tejas Sankar, Mark C Preul, Eric J Kostelich, CJ Thalhauser, and Yang Kuang. Virtual glioblastoma: growth, migration and treatment in a three-dimensional mathematical model. *Cell proliferation*, 42(4):511–528, 2009.

[19] Ferlay J, Ervik M, Lam F, Colombet M, Mery L, Piñeros M, et al. Global Cancer Observatory: Cancer Today. Lyon: International Agency for Research on Cancer, 2020, (accessed February 2021).

[20] Ronald Aylmer Fisher. The wave of advance of advantageous genes. *Annals of eugenics*, 7(4):355–369, 1937.

[21] Ronald Aylmer Fisher. *The genetical theory of natural selection.* , 1958.

[22] CL Frenzen and JD Murray. A cell kinetics justification for gompertz'equation. *SIAM Journal on Applied Mathematics*, 46(4):614–629, 1986.

[23] HP Greenspan. Models for the growth of a solid tumor by diffusion. *Studies in Applied Mathematics*, 51(4):317–340, 1972.

[24] Steven I Hajdu. A note from history: landmarks in history of cancer, part 1. *Cancer*, 117(5):1097–1102, 2011.

[25] Steven I Hajdu. A note from history: landmarks in history of cancer, part 2. *Cancer*, 117(12):2811–2820, 2011.

[26] Steven I Hajdu. A note from history: landmarks in history of cancer, part 3. *Cancer*, 118(4):1155–1168, 2012.

[27] D Hart, E Shochat, and Z Agur. The growth law of primary breast cancer as inferred from mammography screening trials data. *British journal of cancer*, 78(3):382–387, 1998.

[28] E. J. Hinch. *Algebraic equations*, page 1–18. Cambridge Texts in Applied Mathematics. Cambridge University Press, 1991.

[29] Eric C. Holland. Glioblastoma multiforme: The terminator. *Proceedings of the National Academy of Sciences*, 97(12):6242–6244, 2000.

[30] Mohammad Karimi. Diffusion in polymer solids and solutions. *Mass transfer in chemical engineering processes*, 25:17, 2011.

[31] Ardak Kashkynbayev, Yerlan Amanbek, Bibinur Shupeyeva, and Yang Kuang. Existence of traveling wave solutions to data-driven glioblastoma multiforme growth models with density-dependent diffusion. *Mathematical Biosciences and Engineering*, 17(6):7234–7247, 2020.

[32] William Ogilvy Kermack and Anderson G McKendrick. Contributions to the mathematical theory of epidemics. ii.—the problem of endemicity. *Proceedings of the Royal Society of London. Series A, containing papers of a mathematical and physical character*, 138(834):55–83, 1932.

[33] Paul Kleihues, Peter C Burger, and Bernd W Scheithauer. The new who classification of brain tumours. *Brain pathology*, 3(3):255–268, 1993.

[34] Andrei N Kolmogorov. Étude de l'équation de la diffusion avec croissance de la quantité de matière et son application à un problème biologique. *Bull. Univ. Moskow, Ser. Internat., Sec. A*, 1:1–25, 1937.

[35] Mark Kot. *Elements of mathematical ecology*. Cambridge University Press, 2001.

[36] Yang Kuang, John D Nagy, and Steffen E Eikenberry. *Introduction to mathematical oncology*. CRC Press, 2018.

[37] Anna Kane Laird. Dynamics of tumour growth. *British journal of cancer*, 18(3):490, 1964.

[38] Anna Kane Laird. Dynamics of tumour growth: comparison of growth rates and extrapolation of growth curve to one cell. *British Journal of Cancer*, 19(2):278, 1965.

[39] Chong Liu, Jonathan C Sage, Michael R Miller, Roel GW Verhaak, Simon Hippenmeyer, Hannes Vogel, Oded Foreman, Roderick T Bronson, Akiko Nishiyama, Liqun Luo, et al. Mosaic analysis with double markers reveals tumor cell of origin in glioma. *Cell*, 146(2):209–221, 2011.

[40] Alfred James Lotka. *Elements of physical biology*. Williams & Wilkins, 1925.

[41] Suely Kazue Nagahashi Marie and Sueli Mieko Oba Shinjo. Metabolism and brain cancer. *Clinics*, 66:33–43, 2011.

[42] M Marušić. Mathematical models of tumor growth. *Mathematical Communications*, 1(2):175–188, 1996.

[43] JA McCredie. The rate of tumor growth in animals. *Growth*, 29:331–347, 1965.

[44] James D Murray. Vignettes from the field of mathematical biology: the application of mathematics to biology and medicine. *Interface Focus*, 2(4):397–406, 2012.

[45] James Dickson Murray. *MathematicalBiology I. An Introduction*. Springer, 2002.

[46] JD Murray. *Mathematical biology II: spatial models and biomedical applications*, volume 3. Springer-Verlag, 2001.

[47] John A Nelder and Roger Mead. A simplex method for function minimization. *The computer journal*, 7(4):308–313, 1965.

[48] Larry Norton. A gompertzian model of human breast cancer growth. *Cancer research*, 48(24 Part 1):7067–7071, 1988.

[49] Donald M Olsson and Lloyd S Nelson. The nelder-mead simplex procedure for function minimization. *Technometrics*, 17(1):45–51, 1975.

[50] Quinn T Ostrom, Luc Bauchet, Faith G Davis, Isabelle Deltour, James L Fisher, Chelsea Eastman Langer, Melike Pekmezci, Judith A Schwartzbaum, Michelle C Turner, Kyle M Walsh, et al. The epidemiology of glioma in adults: a "state of the science" review. *Neuro-oncology*, 16(7):896–913, 2014.

[51] Ilya Prigogine and Grégoire Nicolis. On symmetry-breaking instabilities in dissipative systems. *The Journal of Chemical Physics*, 46(9):3542–3550, 1967.

[52] Marc R Roussel. Reaction-diffusion equations, 2005.

[53] SI Rubinow. A maturity-time representation for cell populations. *Biophysical journal*, 8(10):1055–1073, 1968.

[54] Timothy S Sadiq and David A Gerber. Stem cells in modern medicine: Reality or myth? *Journal of Surgical Research*, 122(2):280–291, 2004.

[55] Ronald W Shonkwiler and James Herod. *Mathematical biology: an introduction with Maple and Matlab*. Springer Science & Business Media, 2009.

[56] Joel Smoller. *Shock waves and reaction—diffusion equations*, volume 258. Springer Science & Business Media, 2012.

[57] G Gordon Steel. Growth kinetics of tumors. *Cell population kinetics in relation to the growth and treatment of cancer*, pages 59–61, 1977.

[58] Andrew M Stein, Tim Demuth, David Mobley, Michael Berens, and Leonard M Sander. A mathematical model of glioblastoma tumor spheroid invasion in a three-dimensional in vitro experiment. *Biophysical journal*, 92(1):356–365, 2007.

[59] Tracy L Stepien, Erica M Rutter, and Yang Kuang. A data-motivated density-dependent diffusion model of in vitro glioblastoma growth. *Mathematical Biosciences & Engineering*, 12(6):1157, 2015.

[60] Thomas Stiehl and Anna Marciniak-Czochra. Characterization of stem cells using mathematical models of multistage cell lineages. *Mathematical and Computer Modelling*, 53(7-8):1505–1517, 2011.

[61] Akulapalli Sudhakar. History of cancer, ancient and modern treatment methods. *Journal of cancer science & therapy*, 1(2):1, 2009.

[62] Kristin R Swanson, Carly Bridge, JD Murray, and Ellsworth C Alvord Jr. Virtual and real brain tumors: using mathematical modeling to quantify glioma growth and invasion. *Journal of the neurological sciences*, 216(1):1–10, 2003.

[63] Gopal S Tandel, Mainak Biswas, Omprakash G Kakde, Ashish Tiwari, Harman S Suri, Monica Turk, John R Laird, Christopher K Asare, Annabel A Ankrah, NN Khanna, et al. A review on a deep learning perspective in brain cancer classification. *Cancers*, 11(1):111, 2019.

[64] VM Tikhomirov. A study of the diffusion equation with increase in the amount of substance, and its application to a biological problem. In *Selected works of AN Kolmogorov*, pages 242–270. Springer, 1991.

[65] P Tracqui, GC Cruywagen, DE Woodward, GT Bartoo, JD Murray, and EC Alvord Jr. A mathematical model of glioma growth: the effect of chemotherapy on spatio-temporal growth. *Cell proliferation*, 28(1):17–31, 1995.

[66] Rice University. *Concepts of Biology*. OpenStax College, 2013.

[67] Pierre-François Verhulst. Notice sur la loi que la population suit dans son accroissement. *Corresp. Math. Phys.*, 10:113–126, 1838.

[68] E Voit. A first course in system biology, garland science, 2013.

[69] AI Volpert and Vladimir Volpert. Traveling-wave solutions of parabolic systems with discontinuous nonlinear terms. *Nonlinear Analysis, Theory, Methods and Applications*, 49(1):113–139, 2002.

[70] Vito Volterra. Variazioni e fluttuazioni del numero d'individui in specie animali conviventi. 1926.

[71] Ludwig Von Bertalanffy. A quantitative theory of organic growth (inquiries on growth laws. ii). *Human biology*, 10(2):181–213, 1938.

[72] Charles P Winsor. The gompertz curve as a growth curve. *Proceedings of the National Academy of Sciences of the United States of America*, 18(1):1, 1932.

[73] Chuan Xue, Avner Friedman, and Chandan K Sen. A mathematical model of ischemic cutaneous wounds. *Proceedings of the National Academy of Sciences*, 106(39):16782–16787, 2009.

[74] Yanyan Zheng, Helen Moore, Alexandra Piryatinska, Trinidad Solis, and E Alejandro Sweet-Cordero. Mathematical modeling of tumor cell proliferation kinetics and label retention in a mouse model of lung cancer. *Cancer research*, 73(12):3525–3533, 2013.